GA–A22432

THE SPHERICAL TORUS APPROACH TO MAGNETIC FUSION DEVELOPMENT

by
R.D. STAMBAUGH, V.S. CHAN, R.L. MILLER,
P.M. ANDERSON, C.B. BAXI, R.W. CALLIS, H.K. CHIU,
S.C. CHIU, C.B. FOREST, R. HONG, T.H. JENSEN,
L.L. LAO, J.A. LEUER, Y.R. LIN-LIU, M.A. MAHDAVI,
A. NEREM, R. PRATER, P.A. POLITZER, M.J. SCHAFFER,
D.L. SEVIER, T.S. TAYLOR, A.D. TURNBULL,
and C.P.C. WONG

OCTOBER 1996

GA–A22432

THE SPHERICAL TORUS APPROACH TO MAGNETIC FUSION DEVELOPMENT

by
R.D. STAMBAUGH, V.S. CHAN, R.L. MILLER,
P.M. ANDERSON, C.B. BAXI, R.W. CALLIS, H.K. CHIU,
S.C. CHIU, C.B. FOREST, R. HONG, T.H. JENSEN,
L.L. LAO, J.A. LEUER, Y.R. LIN-LIU, M.A. MAHDAVI,
A. NEREM, R. PRATER, P.A. POLITZER, M.J. SCHAFFER,
D.L. SEVIER, T.S. TAYLOR, A.D. TURNBULL,
and C.P.C. WONG

This is a preprint of a paper to be presented at the Sixteenth IAEA International Conference on Plasma Physics and Controlled Nuclear Research, October 7–11, 1996, Montreal, Canada, and to be published in *The Proceedings.*

Work supported in part by
the U.S. Department of Energy
under Grant No. DE-FG03-95ER54309
and GA internal R&D funding

GA PROJECT 4437
OCTOBER 1996

F1-CN-64/G1-2

THE SPHERICAL TORUS APPROACH TO MAGNETIC FUSION DEVELOPMENT

ABSTRACT

The low aspect ratio tokamak or spherical torus (ST) approach offers two key elements needed for an attractive magnetic fusion development path: a low cost, low power, small size market entry vehicle and a strong economy of scale in larger devices. In our studies of the ST approach, we found a very small device (A = 1.4, major radius about 1 m, similar size to the DIII–D tokamak) that would produce ~800 MW thermal, 160 MW net electric, and would have a gain, defined as Q_{PLANT} = gross electric power over recirculating power, of ~1.7. Such a device would have all the operating systems and features of a power plant and would therefore be acceptable as a pilot plant. At about double the linear dimension of the pilot plant, we find 4 GW thermal power plants with an economically viable Q_{PLANT} = 4–5 but which remain a factor 3 smaller than superconducting tokamak power plants. Large ST power plants might be able to burn the advanced fuel D-He^3 if the copper TF coil can be replaced with a superconducting TF coil and suitable shield.

1. INTRODUCTION

The advantages of the spherical tokamak approach have been discussed for many years [1,2]. In recent years, interest in the ST approach has grown rapidly, spawning a number of workshops [3] and a number of new experimental machine proposals [4–6]. Reference [7] is a valuable review of the field. Some studies projecting the ST approach to burning plasma devices have appeared [8,9].

The ST approach minimizes the size of a tokamak power core by discarding components from the inner side of the plasma: no inboard blanket or shield, no inboard poloidal coil (PF) systems, no Ohmic heating (OH) solenoid, resulting in low aspect ratio tokamaks, with aspect ratio A generally less than 1.5. The only customary tokamak component that remains is a single turn copper toroidal field (TF) coil centerpost. Consequently, the ST shrinks to the absolute minimum size and cost fusion system that is still a tokamak.

The key to the ST approach is that the beta values made possible by the combination of high elongation and low aspect ratio are sufficiently high that limits on the neutron wall loading of the blankets determine the machine size. The fusion power produced far exceeds the Ohmic losses in the copper TF coil. With no OH transformer, the ST devices are of necessity steady-state with full non-inductive current drive. High beta equilibria with self-driven current fractions up to 100% have been calculated. The current drive power and the TF coil Ohmic power remain small enough to project systems with reasonable levels of plant recirculating power. E×B shear stabilization of turbulence will be maximized in the ST. The copper TF coil can be jointed and allows simple full dissassembly for replacement of all components, including the centerpost. Estimates of the increase in resistivity of the centerpost from neutron induced transmutation indicate a multi-year lifetime before replacement. The single turn centerpost requires unusual power supplies (few volts, MA currents) which appear possible. The high power density is a challenge to the divertor.

We find a pilot plant (Fig. 1) the size of the present DIII–D tokamak would still produce some net electric power. At 2–3 times the size of the pilot plant, full 1–2 GW net electric power plants have acceptable economics [10].

2. FUSION POWER AND BETA

A large excess of fusion power P_F must be produced relative to the resistive power in the TF centerpost P_c. We calculated a "centerpost gain" $\left(P_F/P_c\right)$ and looked at optimizations. The centerpost is a straight cylinder of radius R_c and height h_c. No other inboard space allowance is taken. We took as independent variables R_c, aspect ratio A, and elongation κ, since the centerpost power consumption is the main issue and we are interested in optimization of performance versus A. The plasma major radius R_0 and minor radius a are then derived. The centerpost current density J_c defines the problem. The fraction of the centerpost area that is copper is λ.

Using standard forms for the D-T fusion reactivity [11], the optimum D-T mix, $n_D = n_T = 1/2\, n_e$, and parabolic profiles with exponents $S_n = 0.25$ and $S_T = 0.25$ to conform to the pressure profile in stability calculations, we can express the fusion power P_F in terms of the volume average plasma toroidal β_T and the vacuum toroidal field B_T to keep contact with the β-limit scaling for higher aspect ratio tokamaks [12] $\beta_N \equiv \beta_T \Big/ \left(I_p/aB_T\right)$ (%,MA,m,T).

$$P_F = 0.88\left(\beta_T B_T^2\right)^2 V(\mathrm{MW,T,m^3}) \quad . \tag{1}$$

A relation for the β-limit as a function of aspect ratio is needed. Using poloidal circumference = $2\pi a\,[(1+\kappa^2)/2]^{1/2}$, one obtains

$$\beta_T \beta_p = 25\left(\frac{1+\kappa^2}{2}\right)\left(\frac{\beta_N}{100}\right)^2 \quad . \tag{2}$$

Equation (2) squarely puts the major conflict in advanced tokamak design at any aspect ratio. One wants high β_T for fusion power and high β_p for high bootstrap fraction. But β_T and β_p trade-off against each other, given conventional β-limit scaling $\beta_N = \text{constant}$. The way to increase β_T and β_p *simultaneously* is to increase κ and β_N.

3. STABILITY STUDIES

To determine β_N (A), we have explored a range of equilibria at low A varying the pressure profile, the current profile, the plasma shape, and aspect ratio [13]. Equilibria with complete bootstrap alignment were made by constraining the pressure and current profile using the TOQ fixed boundary equilibrium code [14]. Examples of fully aligned bootstrap current with bootstrap fraction f_{bs} 90%–100% at aspect ratio of 1.4 have been obtained.

Stability to ideal kink modes and ballooning modes was evaluated. Kink modes with n = 1, 2, and 3 are stable (GATO [15]) for β_N of 8 or larger with wall stabilization for a moderately placed wall. Higher triangularity δ is more favorable for wall stabilization of low mode number kink modes. Wall stabilization is also required for n = 0 axisymmetric modes. Regarding stability to ballooning modes, two paths were pursued to optimize ballooning stability with fully driven bootstrap current. One used a

finite pressure gradient at the plasma edge p'_{edge} as is usual in DIII–D H–mode. A stable equilibrium with β_N = 10 and finite p'_{edge} (77% of the maximum p') has been found and confirmed by several different codes [13]. A second path optimized β_N with p'_{edge} = 0 through an iterative calculation of marginal stability with variation of the pressure profile while maintaining full bootstrap alignment. Our results show a clear dependence of the β limit on δ and κ. Scanning δ at fixed κ (=2.5), both β_N – and β_T– limits show a maximum at δ = 0.4 owing to the competition between the stabilizing effect of a deeper magnetic well at higher δ and higher edge bootstrap current at lower δ. At fixed δ, both β_N- and β_T- limits increase with κ (Fig. 2). At κ = 3, equilibria with β_N exceeding 8 and β_T exceeding 50% with full bootstrap alignment are stable to n = infinity ballooning modes.

Our stability calculations [13] support a *specific advantage* of low aspect ratio in plasma stability. The function $\beta_N = 12/A$ passes through our theory results at A = 1.4 (Fig. 3) and the center of the range of data from DIII–D [16]; $\beta_N = 6$, more optimistic than our assumed function, has been achieved transiently and is expected to be stable in steady-state in second stable core VH–mode (SSC-VH [17], negative central shear mode [18]).

4. POWER GAIN

In our scoping studies, we used the relation β_N = 12/A in Eq. (2) to allow a tradeoff of β_T and β_p with a basis point at the κ = 3, β_N = 8.6, β_T = 56%,f_{bs} = 100% case in Fig. 2. From a study of the dependence of f_{bs} on density and temperature scale lengths we adopted profiles for which $L_n = L_T$ and for which the pressure profile wasas broad as in the stability results. In this case $f_{bs} = 0.72\ \beta_p/\sqrt{A}$. Using β_N = 12/A in Eq. (2) to eliminate β_T in Eq. (1),

$$\frac{P_F}{P_c} = \frac{(0.88)(0.2)^4 \pi^5 \lambda}{\eta_c} \left(\frac{0.36\left[(1+\kappa^2)/2\right]}{\beta_p} \right)^2 \times J_c^2 R_c^4 \frac{(A-1)^2}{A^7} \quad . \tag{3}$$

This relation implies an optimum aspect ratio of 1.4. The relation [Eq. (3)] shows a very strong economy of scale in the low aspect ratio approach since $P_F/P_c \propto R_c^4$. Shortfalls in plasma parameters which lower P_F/P_c can easily be made up by making the machine only slightly larger.

Since $P_F/P_c \propto J_c^2$, we need to ask what limits J_c? Centerpost cooling is an obvious candidate but turns out to not be restrictive. For a water temperature rise of 100°C, a flow velocity of 10 m/s, and λ = 1/2, we can express $J_c^2\,(\mathrm{MA/m^2}) = 6.2\times10^4/h_c$ [19], which leads to very small machines $(R_c = 0.2\,\mathrm{m})$ with enormous power outputs (11 GW!) and high toroidal field (10 T) devices because the centerpost cooling limit supports J_c as high as 200 MA/m^2. Such machines are unrealistically small; the neutron wall loading would be far beyond what blankets could handle.

5. NEUTRON WALL LOADING LIMITS

A neutron wall loading constraint will be the limiting factor in performance. We take 8 MW/m^2 to be at the high end of possibility. We assumed the neutrons are emitted uniformly onto a sphere of radius $R_0 + 2a$, *i.e.*, the blanket is spaced one minor radius from the edge of the plasma.

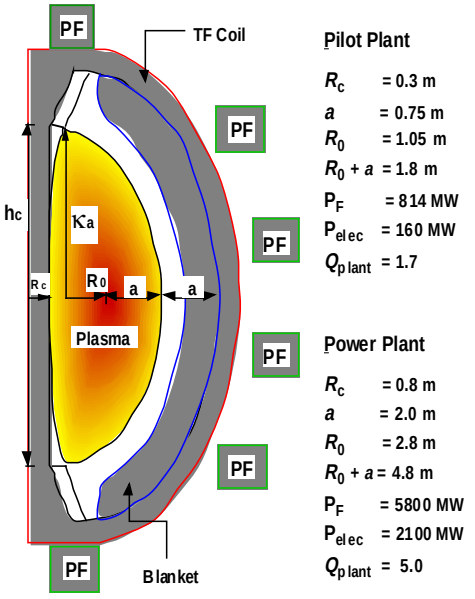

Fig. 1. An ST power plant is 2–3 times the linear dimension of an ST pilot plant. Both cases for A = 1.4, neutron wall load at the blanket 8 MW/m^2, β_T = 62%, β_p = 1.48, f_{bs} = 0.9, κ = 3.0.

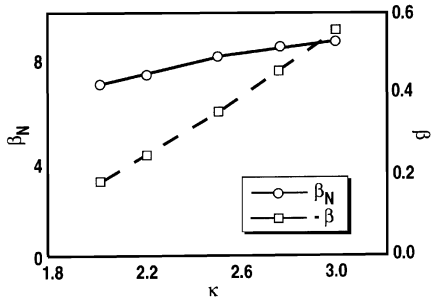

Fig. 2. β and β_N as functions of elongation, κ, δ = 0.4 and A = 1.4.

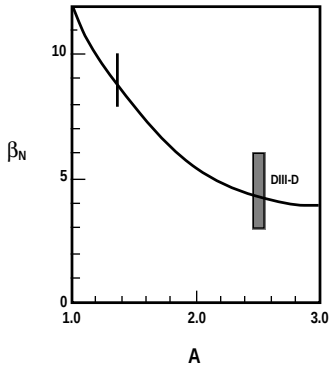

Fig. 3. The relation $\beta_N = 12/A$. Achieved values in DIII–D experiments are shown at A = 2.5. A range of theoretical calculations from Ref. [13] are shown at A = 1.4.

The family of machines with constant wall loading is defined by $J_c^4 R_c^5 =$ constant. With this constraint, the centerpost gain P_F/P_c will have the size scaling $R_c^{3/2}$, much weaker than the R_c^4 scaling considering only operation at the β-limit with a fixed J_C. At the neutron wall loading limit of 8 MW/m^2, we found an interesting family of machines, all of small size, but with high gain and fusion power output.

We found that increasing κ from 2 to 3 is able to effect a factor 2 reduction in plasma and machine volume, providing strong motivation to increase the elongation.

Our choice κ = 3 lies above the passive stability limit [7] but below the feedback stability limit [20].

6. INTEGRATED DESIGNS

We constructed a complete plant model in a spreadsheet. The current density J_c is adjusted to give the specified wall loading power. Some allowance for the elevated operating temperature of the centerpost is made by taking $\eta_c = 2.0\times10^{-2}$ $\mu\Omega$m and we took λ = 0.8. A water flow velocity V_W = 10 m/s always gives a small temperature rise. The twelve outer legs of the TF coil are sized to obtain a resistive dissipation equal to 0.5 of the centerpost power and the resulting cross-sections are modest (0.2 to 0.6 m on a side). The total voltage drop on the TF coil, V_{TF}, ranges from 10 to 7 V.

With semiconductor power supplies for the TF with an internal voltage drop of about 1 V, we take the electrical efficiency of the TF power source to be 0.9 $\left(1-1\mathrm{V}/\mathrm{V}_{\mathrm{TF}}\right)$.

We specify $f_{bs} = 0.9$ and compute $\beta_p = f_{bs}\sqrt{A}/0.72$. The β_T is calculated from Eq. (2) with β_N = 12/A. Then $I_p/aB_T = 100\,\beta_T/\beta_N$ and $I_p(\mathrm{MA}) = aB_T\left(I_p/aB_T\right)$. The safety factor q is always unrestrictive (~6). The product of central density n_0 and temperature T_0 is computed from β_T. We assume T_0 = 30 keV and calculate n_0, which ranges from 3 to 2×10^{20} m^{-3}. These densities range from 0.3 to 0.6 times the Greenwald limit $n_{GR} = I_p(\mathrm{MA})/\pi a^2$.

We compute the power required P_{CD} to drive the remainder of the current $I_{CD} = I_p(1-f_{bs})$ [21]. We compute $P_{CD} = nR_0 I_{CD}/\gamma$, where γ is the usual current drive figure of merit for the various current drive schemes evaluated at the volume average temperature and density [19]. The values P_{CD} were similar for the various rf and NBCD schemes; in our power balance, we used the NBCD result which ranged from 7 to 24 MW.

The electrical efficiency of the current drive system is taken as $\eta_{CD} = 0.4$. All other plant systems are assumed to require 7% of the gross electric power generated. So the power recirculating in the plant is $P_{RECIRC} = P_{CD}/\eta_{CD} + P_{TF}/\eta_{TF} + 0.07P_{GROSS,E}$. A blanket multiplier $M = 1.25$ was taken. None of the power collected as heat $\left(P_\alpha + P_{CD,E} + P_{TF,E}\right)$ was taken into the thermal cycle. The efficiency of the thermal cycle was taken as 46%. The gross electric power is $P_{GROSS,E} = \left[M\left(P_F - P_\alpha\right)\right]/0.46$. $Q_{PLANT} = P_{GROSS,E}/P_{RECIRC}$.

We found the low aspect ratio path does contain a small pilot plant type device and an attractive economy of scale to power plants. All of the designs considered have in common A = 1.4, β_T = 62%, β_p = 1.48, f_{bs} = 0.90, κ = 3.0, neutron power at blanket = 8 MW/m^2.

Figure 4 shows P_F/P_c and Q_{PLANT} versus machine size as gauged by R_c. At the low end, $R_c \sim 0.2$ to 0.3 m, we find pilot plants with $P_F/P_c = 5$ to 10 and $Q_{PLANT} = 1.0$ to 1.7. At larger $R_c = 0.6$ to 0.8 m, we find a suitable range for a power plant with $P_F/P_c = 25$ to 40 and $Q_{PLANT} = 3.8$ to 5.4. The pilot plant makes a fusion power in the range 360 to 800 MW and a net electric power in the range 0 to 160 MW. The power plants make fusion power 3000 to 6000 MW and net electric power in the 1000 to 2000 MW range. These are all small devices. The pilot plant has $R_0 = 0.7$ to 1.0 m and $a = 0.5$ to 0.8 m. The power plants have $R_0 = 2.1$ to 2.8 m and $a = 1.5$ to 2.0 m.

The wall loading constraint forces J_c to decrease as R_c increases as shown in Fig. 5. The pilot plants have $J_c = 90$ to 50 MA/m^2 and toroidal fields 3.2 to 2.9 T. The power plants have $B_0 = 2.4$ to 2.2 T and $J_c \sim 22-16$ MA/m^2, a technically unchallenging value. The centerpost power ranges from 90 MW in the pilot plant to 140 MW in the power plant. The plasma current ranges from 15 MA to 30 MA. The neutral beam current drive power range is from 7 to 24 MW.

Taking account of bremsstrahlung and assuming P_{RAD} = 25% of the sum of $P_\alpha + P_{CD}$, we calculate the index of divertor power handling P/R_0 and find values ranging from 80 to 300 MW/m; P/R_0 in ITER is ~40 MW/m. It appears these devices will need to use a radiating mantle to deliver the power to the large area outer wall instead of trying to handle a majority of the power in the small divertor volume.

7. CONFINEMENT AND E×B SHEAR

We have examined operation at the β-limit. The total heating power $P_\alpha + P_{CD}$ has also been calculated, so we can calculate the energy confinement time required to provide a steady-state at the β-limit. Those confinement times are then compared to

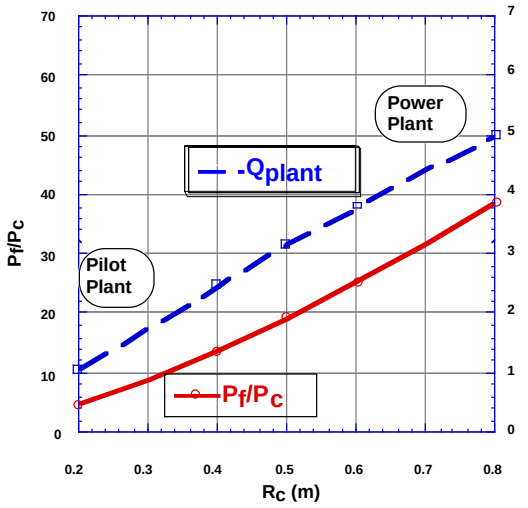

Fig. 4. The ST approach contains a small pilot plant with plant Q = 1–2 and a strong economy of scale to power plants with a plant Q = 4–5.

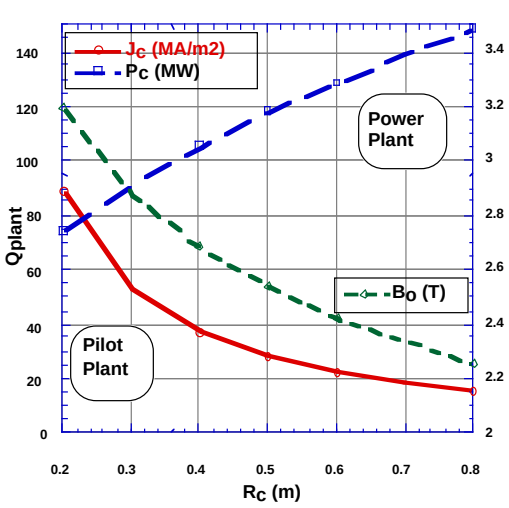

Fig. 5. Allowable neutron wall loading (8 MW/m^2) forces J_c and B_o to decrease with increasing R_c, $\beta_T = 62\%$, $\beta_p = 1.48$, $f_{bs} = 0.9$.

the ITER89–P L–mode scaling [22] to define $H = \tau_E/\tau_{89P}$. The absolute energy confinement times are reasonable, ranging from 0.6 to 1.0 s. An H factor of 5 in the pilot plant range and 3 in the power plant range is required. We note that the H–mode scaling predicts a τ_E about half of L–mode at $A = 1.4$, which makes no sense.

Prospects for obtaining this required confinement quality are excellent. The transport barriers formed in H–mode, VH–mode, and negative central shear (NCS) mode all derive from stabilization of turbulence by sheared E×B flow [23]. Turbulence suppression is strong when the shearing rate [24] exceeds the growth rate of the modes. Assuming isotropy for the turbulence correlation lengths in the plane perpendicular to $\vec{B}$ [24,25] and flat density profiles, the shearing rate is approximately

$$\omega_E = \frac{(RB_\theta)^2}{B}\left|\frac{\partial}{\partial\psi}\left(\frac{E_r}{RB_\theta}\right)\right| \cong \frac{(RB_\theta)^2}{Z_i n_i e B}\frac{\partial^2 P}{\partial\psi^2} \quad (\nabla P \text{ term only}) \quad . \qquad (6)$$

An experimental calibration point is available in that when $\omega_E \gtrsim 100$ kHz, turbulence suppression has been essentially complete, leaving only residual neoclassical transport.

We have evaluated Eq. (6) for ω_E exactly in our highest β equilibrium. Figure 6 shows that ω_E reaches enormous values of 30 MHz in the high pressure gradient region near the outer midplane. Such values are 300 times the 100 kHz values in present experiments that achieve neoclassical transport levels. ω_E is greater than 100 kHz over the outer 20% of the minor radius on the outboard side so a transport barrier with only residual neoclassical transport should form there to support the high pressure gradient this equilibrium requires. Estimates of the confinement times resulting from neoclassical ion heat transport alone exceed our required confinement times by a very large factor.

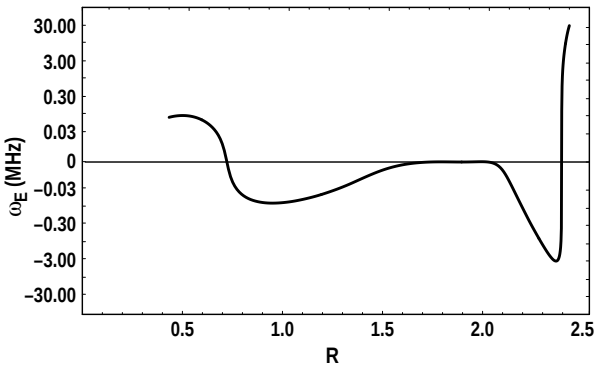

Fig. 6. Turbulence shearing rate versus major radius at the midplane for $n_i = 10^{20}$ m^{-3}.

8. HELICITY INJECTION CURRENT DRIVE

Besides estimating the current drive power from the standard RFCD and NBCD schemes, we also looked at helicity injection current drive derived from an electrode as in the HIT experiment [18]. We estimate the HICD power as ten times the Ohmic dissipation in the plasma assuming a flat current profile in the presence of a temperature profile given by

$$T_e(r) = T_0\left[1-\left(1-T_b/T_0\right)(r/a)^2\right]^{S_T} \quad , \tag{7}$$

$$P_{HICD}\,(\mathrm{MW}) = \frac{0.56\pi R_0 I_{CD}^2\,(\mathrm{MA})}{\pi a^2 \kappa}\,\frac{1}{T_0^{3/2}\,(\mathrm{keV})}\left[\frac{1-\left(T_b/T_0\right)^{1-(3/2)S_T}}{\left(1-\frac{3}{2}S_T\right)\left(1-T_b/T_0\right)}\right] \quad . \tag{8}$$

We have taken $Z_{eff} = 1$. The values P_{HICD} that result for our broad profiles $S_T = 0.25$ with $T_0 = 30$ keV and $T_b = 0.2$ keV are very small, of order 10 kW. In previous studies [10,27] using a peaked profile $S_T = 2$, PHICD ranged from 60 to 100 MW, twice the RFCD and NBCD values. The possible extreme efficiency of HICD for broad T_e profiles warrants further investigation.

9. TECHNOLOGY ISSUES

We calculated the lifetime of the centerpost in the power plant (R_c = 0.6 m case) against the nuclear transmutation induced increase in resistance, using 2-D distributions of dpa calculated in an R_c = 0.14 m centerpost [26] adapted to our larger centerpost. One MW-yr/m^2 produces 10 dpa in the copper surface at the midplane. The change in resistivity per dpa is 2.8×10^{-10} Ω-m/dpa. With an 8 MW/m^2 neutron flux on the centerpost, we find a 10% increase in resistance in one year, 50% increase in 7 years, and a 100% increase in 22 years. The centerpost changeout time for economic reasons (too high P_c) would be ~7 years.

We also looked at the unusual low voltage, high current semiconductor power supplies needed for the one turn in each return leg TF coil. To keep reasonable the transmission line power losses, the power supplies must closely ring the device (5 m

transmission line lengths) with a floor space requirement of 0.3 m^2/MVA and a 6 m height. The cost for a 12 return leg system for the power plant is about \$70M–\$110M.

10. PROSPECTS FOR ADVANCED FUEL BURNING

Because of the strong scaling of gain P_F/P_c with size ($\alpha\ R_c^4$), the question naturally arises as to whether there is enough excess capacity in the ST at large size to burn advanced fuels like D-He^3 despite their lower reactivity. A D-He^3 system can produce as low as 1% of the neutrons from a D-T system, effectively removing centerpost radiation damage as a design issue. We developed the formula for fusion power from D-He^3 [27] in terms of β and obtained $P_F = 0.016\ \left(\beta_T\ B_T^2\right)^2\ V$ (MW, T, m^3).

The basic difficulty with realizing an effective D-He^3 system is a surprising one; for systems with high gain, the absolute value of the fusion power produced is too large. The D-He^3 fusion power output is 55 times less than the D-T output at the same β_T. To get the same gain P_F/P_c we must increase the size of the machine like $R_c\ \alpha\ (55)^{1/4}$. But P_F scales like R_c^7. Hence the ratio of P_F in our larger D-He^3 device to P_F in our smaller D-T power plant will be

$$\frac{P_{D-He^3}}{P_{D-T}} = \frac{1}{55}\left[(55)^{1/4}\right]^7 = (55)^{3/4} = 20 \quad . \tag{9}$$

We get 20 times more fusion power out at the same gain P_F/P_c!

We have not been able to find a sensible set of parameters for a copper TF coil ST burning D-He^3. One is led to large devices with a very large centerpost $R_c \sim 3$ m and extremely low $J_c \sim 6$ MA/m^2. Within the space envelope afforded by $R_c = 3$ m one could replace the copper TF coil with a superconducting TF coil and include a cryostat and neutron shield. This step eliminates the ohmic dissipation in the TF from the power balance and allows a plant Q = 4.3. Parameters of copper and superconducting D-He^3 systems are given in Table I.

We also looked at D-T systems in the large sizes required to shield a superconducting centerpost (Table I). The endpoint of a copper TF ST development path starting at small $R_c = 0.3$ m pilot plants could be superconducting STs with $R_c >$ 1.5 m.

11. SUMMARY AND CONCLUSIONS

We examined the ultimate performance of the ST at its beta limit and the neutron wall loading limit at the blanket. Full stability calculations at A = 1.4 found $\beta_N = 8$ to 10 with 100% fully aligned bootstrap current.

We demanded a 90% bootstrap fraction. We calculated the current drive power requirements for the various standard schemes to drive the remaining 10% of the current. We performed basic physics studies of FWCD in the low A regime. We also evaluated helicity injection current drive.

We evaluated the energy confinement required to reach the β_T limit. We found that owing to the high $\beta\ B_T$ product in the ST the stabilization of turbulence by sheared E×B flow should be one to two orders of magnitude greater than in existing devices which are seeing only residual neoclassical transport in their transport barriers.

We found systems with the centerpost gain P_F/P_c greater than 20 and a strong size dependence $\left(R_c^4\right)$ of the gain. The cooling of the centerpost imposes no meaningful

Table I
Devices at an 8 MW/m^2 Neutron Wall Load

	D-He^3		D-T
Parameter	Copper	Superconducting	Superconducting
R_c (m)	3	1.5	1.5
R_0 (m)	10.5	5.25	5.25
a (m)	7.5	3.75	3.75
J_c (MA/m^2)	6	$\gtrsim 60^*$	$\gtrsim 60^*$
Fusion power (MW)	23,000	1,400	10,000
Q_{PLANT}	3.4	4.3	12
Net electric power (MW)	7,600	500	4,200
Current drive power (MW)	105	42	30
I_P (MA)	175	73	44
B_0 (T)	3.2	2.7	1.6
τ_E (s)	5.7	8.1	2.1
H	2.1	4.5	2.4
P_F/A_{wall} (MW/m^2)	5.7	1.4	4.0†
T_0 (keV)	100	60	30
n_0 (10^{20} m^{-3})	1.4	1.7	1.0

*Assuming one meter thick neutron shield.
†Neutron power at the blanket.

restriction on the design of ST machines. The high beta potential of the ST is so great that the neutron flux into the fusion blankets was found to limit the size of the device. An aggressive assumption of 8 MW/m^2 at the blanket then led to the small pilot plant and power plant possibilities that we have found.

We found an acceptable centerpost lifetime against transmutation induced resistance increase and an acceptable technical path to the low voltage, high current TF power supplies.

We found the possibility of D-He^3 burning devices at large size $R_c > 1.5$ m with a superconducting TF centerpost and suitable shield.

The pilot plant is the key to the ST fusion development path. It appears possible to design a pilot plant that would only be the size of the present DIII–D tokamak and yet still produce 0–160 MW net electric. The plant Q, defined as the ratio of gross electric power to internal recirculating power is only 1–2. The low plant Q will be acceptable in a pilot plant if the concept has a strong economy of scale. The ST size scaling is very strong; the ratio of fusion power to the Ohmic dissipation in the copper TF coil magnet scales as the fourth power of the linear dimension. Consequently, we easily found small power plants with economically acceptable recirculating power (plant Q ~ 4–6, net electric power 1–2 GW) just by doubling the linear dimensions of the device with no changes in technology. The ST is a simplified tokamak with no hard to service inboard blankets, shields, PF or OH coils. Because the TF coil is copper, it can be jointed and so afford easy complete dissassembly of the machine for service. The ST concept offers high elongation and a natural divertor without a divertor coil. Finally, because the ST pilot plant is a full net electric and tritium producer, it will provide a full exercise of the siting and licensing process, but again at a low cost, low financial risk scale. The fact that a viable concept for a pilot plant exists is the principal attraction of the ST approach to fusion development.

12. REFERENCES

[1] PENG, Y-K.M., and STRICKLER, D.J., Nucl. Fusion **26** 769 (1986).
[2] PENG, Y-K.M., and HICKS, J.B., "Engineering Feasibility of Tight Aspect Ratio Tokamak (Spherical Torus) Reactors," *Proc. of the 16th Symposium on Fusion Technology*, London, September 3–7, 1990.
[3] PENG, Y-K.M., et al., Fusion Technol. **29** 210 *(*1995).
[4] DARKE, A.C. et al., "The Mega Amp Spherical Tokamak," *Proc. of the 16th Symposium on Fusion Energy*, Champaign-Urbana, Illinois, 1995.
[5] CHRZANOWSKI, J.H., et al., "Engineering Overview of the National Spherical Tokamak Experiment," *ibid*.
[6] FRC STAFF "USTX — The University Spherical Tokamak Experiment," DOE/ER/542-41-159 (1996).
[7] SYKES, A., Plasma Phys. and Contr. Fusion **36** B93 (1994).
[8] PENG, Y-K.M., et al., in *Proc. of the 15th Int. Conf. on Plasma Physics and Controlled Nuclear Fusion Research*, Seville, Spain, 1994 (International Atomic Energy Agency, Vienna, 1995) Vol. 2, p. 643.
[9] HENDER, T.C. et al., *ibid*.
[10] STAMBAUGH, R.D., et al., "The Spherical Tokamak Path to Fusion Power," General Atomics Report GA-A22226 (1996) submitted to Fusion Technology.
[11] *NRL Plasma Formulary* NRL/PU/6790-94-265, J. D. Huba, editor (1994).
[12] CALLEN, J.D., et al., Phys. Today **45** 34 (1992).
[13] MILLER, R.L., et al., "Stability for Bootstrap-Current Driven Low Aspect Ratio Tokamaks," General Atomics Report GA-A22321, submitted to Phys. of Plasmas.
[14] MILLER, R.L., and VANDAM, J.W., Nucl. Fusion **28** 2101 (1987).
[15] BERNARD, L.C., et al., Comput. Phys. Commun. **24** 377 (1981).
[16] FERRON, J.R., et al., Phys. Fluids **B 5** 2532 (1993).
[17] STAMBAUGH, R.D., et al., Plasma Phys. and Contr. Nucl. Fusion Research **1** 83 (1994).
[18] LAZARUS, E.A., et al., "Higher Fusion Power Gain With Pressure Profile Control in Strongly-Shaped DIII–D Tokamak Plasmas," General Atomics Report GA–A22292 (1996) submitted to Phys. Rev. Let*t*.
[19] MONTGOMERGY, D.B., *Solenoid Magnet Design,* (Wiley-Interscience, New York, 1972).
[20] STAMBAUGH, R.D., et al., Nucl. Fusion **32** 1642 (1992).
[21] TONON, G., "Current Drive Efficiency Requirements for an Attractive Steady-State Reactor," *Proc. of the Workshop on Tokamak Concept Improvement*, Varenna, Italy, August 1994, p. 233.
[22] YUSHMANOV, P.N., et al., Nucl. Fusion **30** 1999 (1990).
[23] DOYLE, E.J., et al., paper IAEA F1-CN-64/A6-4, this conference.
[24] HAHM, T.S., and BURRELL, K.H., Phys. Plasmas **2** 1648 (1995).
[25] HAHM, T.S., and BURRELL, K.H., private communication.
[26] CHENG, E.T., et al., "Study of a Spherical Tokamak Based Volumetric Neutron Source," TSIR-45 (1996).
[27] MILEY, G.H., TOWNER, H., IVICH, N., "Fusion Cross Sections and Reactivities," University of Illinois Report COO-2218-17, June 1994.